ARTICLE

Structural Integrity Analysis of Containers Lost at Sea Using Finite Element Method

Selda Oterkus[1]   Bingquan Wang[1]   Erkan Oterkus[1*]   Yakubu Kasimu Galadima[1]   Margot Cocard[1]
Stefanos Mokas[2]   Jami Buckley[2]   Callum McCullough[3]   Dhruv Boruah[4]   Bob Gilchrist[4]

1. PeriDynamics Research Centre, Department of Naval Architecture, Ocean and Marine Engineering, University of Strathclyde, Glasgow, UK
2. Buckley Yacht Design Ltd, New Milton, UK
3. M Subs Limited, Plymouth, UK
4. Oceanways Technologies Ltd, London, UK

ABSTRACT

Unlike traditional transportation, container transportation is a relatively new logistics transportation mode. Shipping containers lost at sea have raised safety concerns. In this study, finite element analysis of containers subjected to hydrostatic pressure, using commercial software ANSYS APDL was performed. A computer model that can reasonably predict the state of an ISO cargo shipping container was developed. The von Mises stress distribution of the container was determined and the yield strength was adopted as the failure criterion. Numerical investigations showed that the conventional ship container cannot withstand hydrostatic pressure in deep water conditions. A strengthened container option was considered for the container to retain its structural integrity in water conditions.

1. Introduction

As a light steel structure, containers have many advantages in ocean transportation. Container transportation reduces the number of manual loading and unloading, and handling in traditional transportation methods, which can avoid cargo damage, wet damage, and loss caused by human and natural factors. Therefore, the shipping container transportation method has completely replaced the traditional shipping method and has become a new and highly efficient transportation method [1].

Container transportation has revolutionized the transportation of goods by sea and has become the global standard for transportation of goods in the world today.

---

*Corresponding Author:
Erkan Oterkus,
PeriDynamics Research Centre, Department of Naval Architecture, Ocean and Marine Engineering, University of Strathclyde, Glasgow, UK;
Email: erkan.oterkus@strath.ac.uk*

Although containers simplify the transportation of large quantities of goods, many accidents still occur during transportation, causing a large number of containers to be lost during sea transportation. The World Shipping Council's 2020 Sea Container Lost Report shows that an average of 1,382 containers are lost at sea each year [2]. According to "Safety and Shipping Review" by Allianz. Although it is not uncommon for containers to be lost at sea, the risks of bad weather, improper stowage and strapping, and even the resulting environmental issues have caused people to pay additional attention to the issue of container loss [3].

Containers are usually manufactured in factories, transported to the construction site, and assembled quickly [4]. Due to the rapid increase in the use of freight containers for marine cargo and the development of special container ships, the safety of containerization in marine transport has been considered by International Organization for Standardization (ISO). Consequently, International Convention for Safe Containers (CSC) was introduced which aims to sustain a high level of safety of human life and facilitate international transport of containers by providing uniform international safety regulations [5].

There have been various studies available in the literature which considers the structural analysis of containers. Giriunas et al. [6] have investigated the ISO shipping container's structural strength for non-shipping applications. Antoniou and Oterkus [7] proposed origami based design concepts which can improve the structural efficiency of a container by FEM. An analytical, numerical, and experimental work on the in-plane stiffness of container buildings has been carried by Zha and Zuo [4]. They presented a feasible design and construction of the container. However, there is no study available in the literature which investigates the state of the containers lost at sea.

The main goal of this study is to analyse structural integrity of the International Organization for Standardization (ISO) shipping containers lost at sea. The construction standards of containers are presented. The structural response of shipping container subjected to underwater hydrostatic loading conditions is investigated. The von Mises stress distribution on a container at various water depths is demonstrated. Strengthened container option to withstand higher hydrostatic pressures is investigated.

2. Methodology

2.1 Finite Element Method

In this study, a standard shipping container model was constructed and analysed by using finite element method. For numerical calculations, ANSYS, a commercial finite element software, was utilised. The container is subjected to hydrostatic pressure around all surfaces, which represents the state of the container lost at sea. The thickness of the side and top walls of the container is significantly smaller compared to its length and width. Consequently, the container was discretized by shell elements in the finite element model. The thickness of the plates can be defined through the section property definition.

The element type, SHELL181, used in this work is widely used to simulate shell structures with thin to medium thickness. As presented in Figure 1, it is a four-node element with six degrees of freedom at each node which are translations in the x, y, and z directions, and rotations about the x, y, and z-axes.
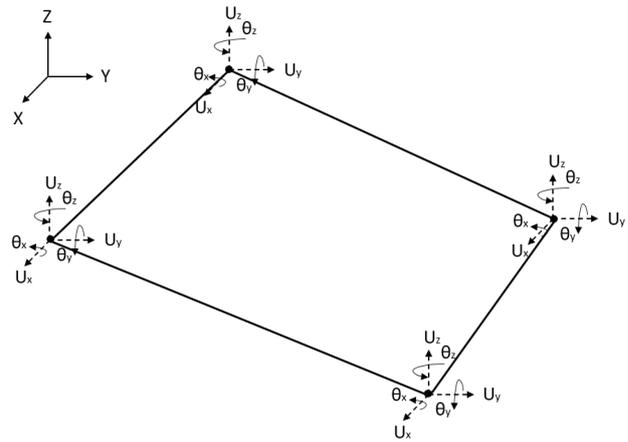

Figure 1. SHELL181 Geometry and Its Nodal Degrees of Freedom.

2.2 Failure Criterion

In this study, the structural integrity of the container was examined by using the von Mises yield criterion. It was assumed that if the von Mises stress of the container subjected to hydrostatic loading is equal or greater than the yield limit of the construction material, then the container will damage.

The stress state at a point can be defined by a 3×3 tensor for a three-dimensional model as

$$\begin{bmatrix} \sigma_{xx} & \sigma_{xy} & \sigma_{xz} \\ \sigma_{xy} & \sigma_{yy} & \sigma_{yz} \\ \sigma_{xz} & \sigma_{yz} & \sigma_{zz} \end{bmatrix} \tag{1}$$

where σ_{xx}, σ_{yy}, σ_{zz} are normal stresses and σ_{xy}, σ_{xz}, σ_{yz} are shear stresses. Von Mises stress σ_v combines the stress components or principal stresses into equivalent stress. In terms of stress components given in Equation (1), it can be calculated as [8]

$$\sigma_v = \sqrt{\frac{(\sigma_{xx} - \sigma_{yy})^2 + (\sigma_{yy} - \sigma_{zz})^2 + (\sigma_{zz} - \sigma_{xx})^2 + 6(\sigma_{xy}^2 + \sigma_{yz}^2 + \sigma_{zx}^2)}{2}} \tag{2}$$

In terms of principal stresses, it can be expressed as [8]

$$\sqrt{\frac{(\sigma_1 - \sigma_2)^2 + (\sigma_2 - \sigma_3)^2 + (\sigma_3 - \sigma_2)^2}{2}} \qquad (3)$$

in which σ_1, σ_2 and σ_3 are principal stresses.

3. Container Geometry Model

Depending on the types of goods that their containers are carrying, ISO and CSC stipulate specifications related with structural strength, applicability, and application of shipping containers. According to the guidance based on ISO, CSC, and container manufacturer standards, the dimensions of the most common 20 ft container are shown in Table 1 and Figure 2.

Table 1. The geometrical dimensions of a 20 ft container

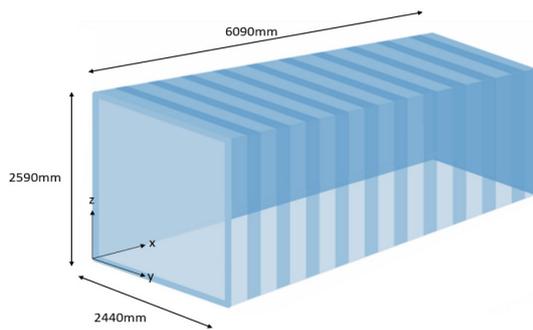|	Length L	Width W	Height H
20 ft container	6090 mm	2440 mm	2590 mm

Figure 2. Dimensions of a 20 ft shipping container.

The container was designed and constructed for the transportation of general cargo on sea. The main components of the container in this work focused on the side walls, end walls and the roof of the container. The trapezium section sidewall is built with 9Pcs 2.6 mm thick fully vertically continuous corrugated steel panels at the intermediate area and 2Pcs 2.6 mm thick fully vertically continuous corrugated steel panels at both ends. The top to bottom view of the side wall is presented in Figure 3.
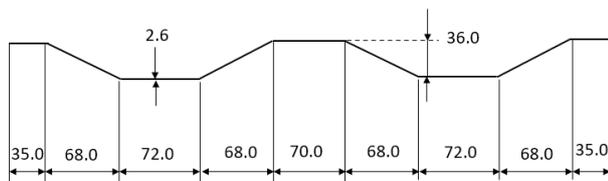

Figure 3. Top to bottom view of the side wall.

The trapezium section end wall in Figure 4 was constructed with 2.6 mm thick vertically corrugated steel panels, which are butt welded together to form one panel.
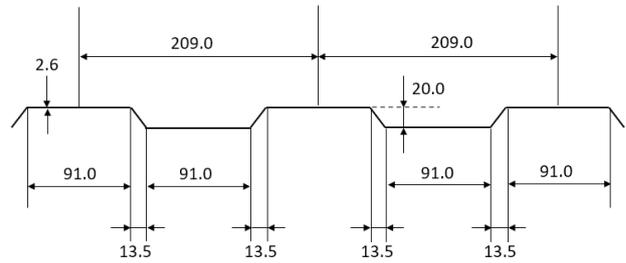

Figure 4. Top to bottom view of the end wall.

The roof was constructed by several die-stamp corrugated steel sheets with a certain upwards camber at the centre of each trough and corrugation while the floor of the container was constructed as a flat sheet.

4. Numerical Evaluation

Finite element software Ansys Mechanical APDL was performed for finite element analysis in this study. The considered container shown in Figure 5 was constructed based on the geometry from Table 1. The side walls are constructed based on the dimensions provided in Figure 3 and Figure 4, respectively.
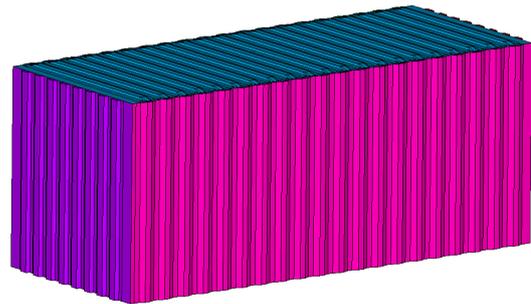

Figure 5. The model geometry of the container.

The container components are typically constructed with steel plate. The density ρ, elastic modulus E and Poisson's ratio v of the model are specified as $\rho = 7850$ **kg/m³**, $E = 200$ **Gpa**, and $v = 0.3$. The material parameter and constitutive relationship of the container model varies depend on the material selected as three types of widely used metal material was considered in the construction. Table 2 indicates material properties of these three material types including ASTM A283 carbon steel [9], SPA-H steel [10] and HY-100 [11] steel.

Table 2. Material parameters of container model

Material Type	Yield Strength σ_{yield}(Mpa)	Ultimate Strength σ_s(Mpa)
ASTM A283	165	310
SPA-H	457	572
HY-100	744	1062

The element size, element shape and mesh type of each component in the container model are specified in Table 3. It is worth noting that to make sure that all components are connected to each other. It is important to merge co-incident nodes after the mesh generation is completed, which can tie separate but coincident parts of the model together.

The container model is considered in the occasions of falling and lost at sea during the operation caused by the un-expected sea state (Figure 6). The container is subjected to hydrostatic pressure. Defining the density of the seawater as ρ_s =1025 $\mathbf{kg/m^3}$, the state of the container was investigated at different water depths. The pressure values at different water depths are shown in Table 4. The pressure loading is applied on all surfaces of the container model in the analysis. In finite element model, the hydrostatic pressure was considered as surface loads and applied on nodes.
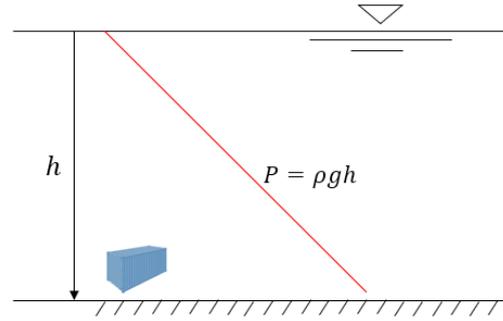
Figure 6. Schematic drawing of container lost at sea and associated hydrostatic pressure acting on it.

The constrained displacements were applied as boundary conditions on the container model to prevent rigid body motion. In addition to hydrostatic pressure acted on all surfaces of the container components, the constrained displacements on the container surface were specified as

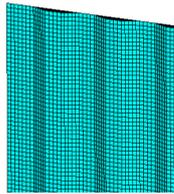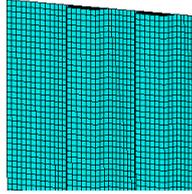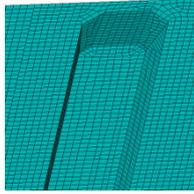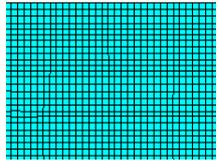**Table 3.** The details of the finite element model of the container

Component	Side Wall	End Wall	Top Roof	Bottom Floor
Mesh Form				
Element Type	Shell 181			
Size	18 mm	18 mm	10 mm	14 mm
Mesh Type	Structured	Structured	Structured	Structured
Thickness	2.6 mm	2.6 mm	3 mm	20 mm

Table 4. Hydrostatic pressure at different water depths.

Depth (m)	Pressure (Pa)
5	50276.25
15	150828.75
30	301657.5
50	502762.5

$$u_x\left(x=\frac{L}{2},y=0,z=\frac{H}{2}\right)=u_z\left(x=\frac{L}{2},y=0,z=\frac{H}{2}\right)=0 \qquad (4)$$

$$u_x\left(x=\frac{L}{2},y=W,z=\frac{H}{2}\right)=u_z\left(x=\frac{L}{2},y=W,z=\frac{H}{2}\right)=0 \qquad (5)$$

$$u_x\left(x=\frac{L}{2},y=\frac{W}{2},z=H\right)=u_y\left(x=\frac{L}{2},y=\frac{W}{2},z=H\right)=0 \qquad (6)$$

$$u_x\left(x=\frac{L}{2},y=\frac{W}{2},z=0\right)=u_y\left(x=\frac{L}{2},y=\frac{W}{2},z=0\right)=0 \qquad (7)$$

in which u_x, u_y and u_z are the displacements in x, y and z directions, respectively.

5. Results and Discussion

The von Mises stress distribution on the container at considered depths is presented in Figure 7. High von Mises stresses can be observed in the middle of the sidewalls. Moreover, a relatively high von Mises stress distribution is shown on the edges of the container model. According to the failure criterion defined by the yield strength and considered construction materials in Table 2, the maximum von Mises stress observed on the container exceeds the yield strength at all water depths. Therefore, the watertightness and structural integrity cannot be maintained after conventional shipping containers are lost at sea.

Based on the conclusion from the comparison, the container needs to be strengthened to withstand hydrostatic pressure. Considering the containers are designed to be heavily loaded and stacked with other containers, it is not feasible to change the geometrical design of the container as this will cause the re-designed container incompatible

with other containers operating in the market. However, the container strength can be improved by increasing the thickness of the sidewalls or alternative construction material. Therefore, in the second case study, the container model components have been redesigned with a different thickness. The new thickness assigned to each component is shown in Table 5. The second case has identical mesh configuration, loading conditions, and constrained displacements with the formal case.

Table 5. The thickness of re-designed container components

Component	Side Wall	End Wall	Top Roof	Bottom Floor
Thickness	22 mm	22 mm	26 mm	30 mm

Figure 8 presents the distribution of von Mises stress of the re-designed container. The comparison between maximum von Mises stress at various depths and yield strength for selected materials is shown in Figure 9. The maximum von Mises stress of the container model is lower than the yield strength of all three materials considered in this study. Thus, the new container design can retain the structural integrity of the container in deeper water conditions.

Table 6 compares the effect of thickness on the maximum von Mises stress between the original and thickened container at different water depths. It can be observed that the thickened container significantly reduces the maximum von Mises stress when subjected to the same hydrostatic pressure conditions as the conventional container.
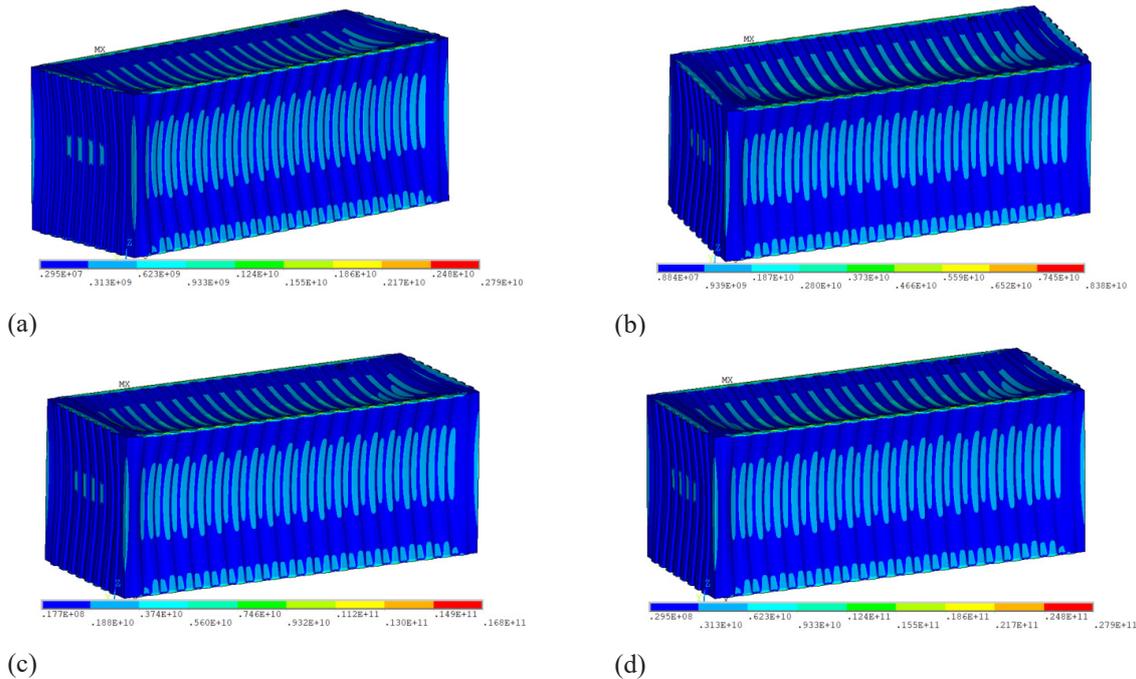

(a)

(b)

(c)

(d)

Figure 7. von Mises stress distribution on the container at (a) 5 m, (b) 15 m, (c) 30 m,(d) 50 m water depths.
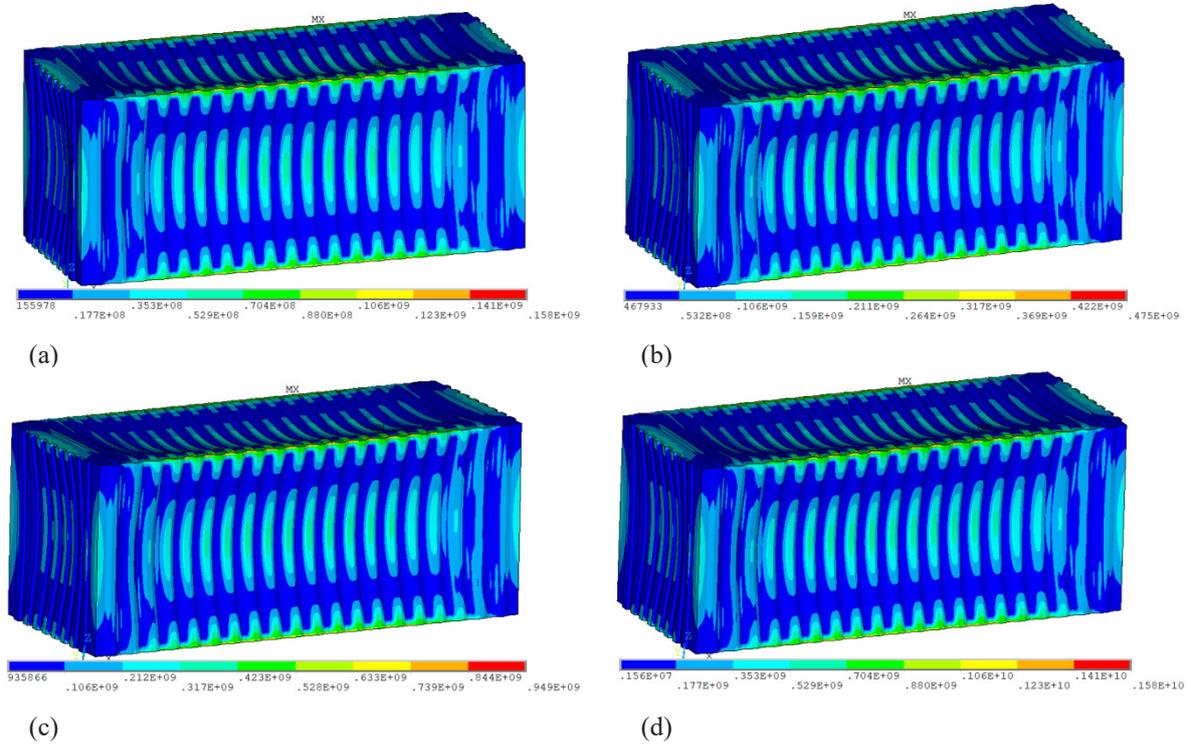
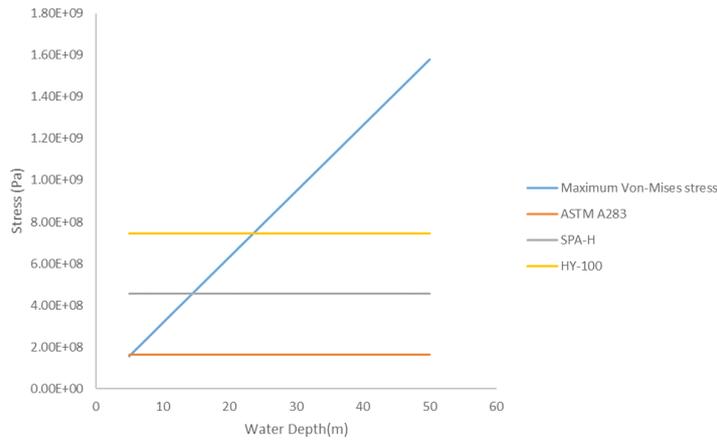**Figure 8.** von Mises stress distribution of re-designed container at (a) 5 m,(b) 15 m,(c) 30 m,(d) 50 m.

Figure 9. The comparison between maximum Von-Mises stress at various depths and yield strength.

Table 6. The effect of thickness on maximum Von Mises stress

Water Depth	Original Configuration	Thicker Configuration	Stress Reduction
5 m	2.79E9 Pa	1.58E8 Pa	94%
15 m	8.38E9 Pa	4.75E8 Pa	94%
30 m	1.68E10 Pa	9.49E8 Pa	94%
50 m	2.79E10 Pa	1.59E9 Pa	94%

6. Summary and Conclusions

In this study, finite element analysis was conducted to investigate the structural behaviour of shipping containers lost at sea. Three different construction materials were discussed for conventional size containers. von Mises stress was employed as a failure criterion. The hydrostatic pressure was increased with the water depth. For containers constructed with traditional configuration, the container lost its structural integrity in shallow water very quickly. The increased thickness reduced the von Mises stress and made the container to retain its structural integrity at a deeper water level.

Unpredictable weather conditions and low operational risk awareness could cause shipping containers to be lost at sea. Increasing the thickness of the container sidewall will increase production costs, but if the structure is damaged when fell into the water, the consigned goods may spread out in the sea and float. Floating containers and consignments could pose a risk of collision with small ocean-going vessels such as yachts and fishing boats. Moreover, if the container contains dangerous goods that may cause risk to the ecological environment, it is even more important to maintain the structural integrity of the container when it falls into the water to prevent any type of pollution. As an alternative solution to traditional container shipping, commercial type cargo submarines can be utilised especially for short distances.

Acknowledgement

Conflict of Interest

There is no conflict of interest.

References

[1] Lee, C.Y., Song, D.P., 2017. Ocean container transport in global supply chains: Overview and research opportunities. Transportation Research Part B: Methodological. 95, 442-474.

[2] The International Institute of Marine Surveying (IIMS), 2020. World Shipping Council containers lost at sea 2020 report issued and shows a decrease. [online] Available at: <https://www.iims.org.uk/world-shipping-council-containers-lost-at-sea-2020-report-issued-and-shows-a-decrease/> (Accessed 29 December 2021).

[3] Allianz, 2021. Safety and Shipping Review. An annual review of trends and developments in shipping losses and safety.

[4] Zha, X., Zuo, Y., 2016. Theoretical and experimental studies on in-plane stiffness of integrated container structure. Advances in Mechanical Engineering. 8(3), 1687814016637522.

[5] CSC, 1996. International convention for safe containers.

[6] Giriunas, K., Sezen, H., Dupaix, R.B., 2012. Evaluation, modeling, and analysis of shipping container building structures. Engineering Structures. 43, 48-57.

[7] Antoniou, K., Oterkus, E., 2019. Origami influence on container design. *A*nnals of Limnology and Oceanography. 4(1), 015-019.

[8] Timoshenko, S.P., Goodier, J.N., 1951. Theory of elasticity.

[9] ASTM International, 2013. ASTM A283/A283M-13-Standard Specification for Low and Intermediate Tensile Strength Carbon Steel Plates.

[10] Akkaş, N., 2017. Welding time effect on tensile-shear loading in resistance spot welding of SPA-H weathering steel sheets used in railway vehicles. Acta Physica Polonica A. 131(1), 52-54.

[11] Zarzour, J.F., Konkol, P.J., Dong, H., 1996. Stress-strain characteristics of the heat-affected zone in an HY-100 weldment as determined by microindentation testing. Materials characterization. 37(4), 195-209.